Proceedings of the XVIII ECSMGE 2024
GEOTECHNICAL ENGINEERING CHALLENGES
TO MEET CURRENT AND EMERGING NEEDS OF SOCIETY

ISBN 978-1-032-54816-6
DOI 10.1201/9781003431749-527

ECSMGE 24
XVIII EUROPEAN CONFERENCE ON SOIL MECHANICS AND GEOTECHNICAL ENGINEERING

Groundwater in geosynthetics-reinforced pile-supported embankments, 3D Experiments

Nappe phréatique affleurant les remblais renforcés par géosynthétiques sur pieux, Expérimentations en 3D

S.J.M. van Eekelen*, B. Wittekoek, R.A. Zwaan, A. Bezuijen
Deltares, Delft, Netherlands

A. Nancey
Solmax, Paris, France

**suzanne.vaneekelen@deltares.nl*

ABSTRACT: This paper investigates the influence of groundwater on geosynthetic-reinforced pile-supported (GRPS) embankments. 3D experiments showed that groundwater primarily reduces the load, mainly through uplift forces, but also causes a slight reduction in soil arching. However, the soil arching quickly recovers when the groundwater level decreases again. The Concentric Arches (CA) model (CUR226, 2016), combined with Archimedes' principle, provides the most accurate match compared to two other main calculation models. No significant correlation between groundwater levels and geosynthetic reinforcement strains was observed.

RÉSUMÉ: Cet article examine l'impact du niveau de la nappe phréatique sur les remblais renforcés par des géosynthétiques et des pieux (GRPS). Les expériences 3D montrent que la présence d'eau réduit principalement la charge par des forces de soulèvement, avec une légère réduction de l'effet de voûte de sol. Cependant, cet effet se rétablit rapidement lorsque le niveau d'eau souterraine diminue. Le modèle des arcs concentriques (CA) (CUR226, 2016), combiné avec le principe d'Archimède, offre la meilleure correspondance parmi les modèles de calcul. Aucune corrélation significative entre les niveaux d'eau et les déformations du renforcement géosynthétique n'a été observée.

Keywords: Groundwater; geosynthetic-reinforced pile-supported embankments; soil arching.

1 GROUNDWATER IN GEOSYNTHETIC-REINFORCED PILED EMBANKMENTS

The calculation model in the CUR226 (2016) design guideline for geosynthetic-reinforced pile-supported (GRPS) embankments was validated with over 100 measurements in experiments and field (van Eekelen et al., 2015). The validated application of a guideline is limited to circumstances like the ones from which the validation measurements were obtained. For GRPS embankments, this means for example that the entire embankment must be located above the groundwater table.

However, infrastructure needs to remain usable during or after heavy rain. In addition to that, in low, flat, subsidence-prone areas, it is often desirable to install the embankment at least partly below groundwater level. Therefore, insight is required in the influence of groundwater on the behaviour of GRPS embankments.

Limited research was done on the influence of water in a piled embankment. Briançon and Simon (2012), Sloan (2011), and Van Eekelen et al. (2020) observed that heavy rainfall affects measurements.

Song et al. (2018) presented small-scale 2D trapdoor tests with sand and concluded that water can degrade the soil arching. Wang et al. (2019), however, showed with full-scale 3D model experiments that the soil arching strengthened with an increasing water level.

In contrast, Van Eekelen et al., (2023) found no significant correlation between the groundwater table and GR strains during four years monitoring in a partly submerged GRPS embankment.

Various mechanisms can play a role when the groundwater rises in a GRPS embankment:

- An increase in uplifting forces, resulting in a reduction of effective stress. This study investigates whether this affects the soil arching mechanism, deformations and GR tensile strains.
- Swelling of the subsoil underneath the reinforcement, as measured by van Eekelen et al. (2020). The subsoil swelling reduces strain

in the reinforcement and the load on the piles. This situation is not addressed in this study.

- Dynamic liquefaction. It is essential to determine whether fill layers in the design may be liquefiable. This phenomenon is also not considered in this study.

The study aims to investigate the influence of high and changing groundwater levels in a GRPS embankment, addressing the following questions: How does the changing groundwater table in a GRPS embankment affect the soil arching in the fill, the deformations and the GR strains? For this purpose, the paper presents 3D laboratory experiments, analyses the results, and compares these with analytical calculations.

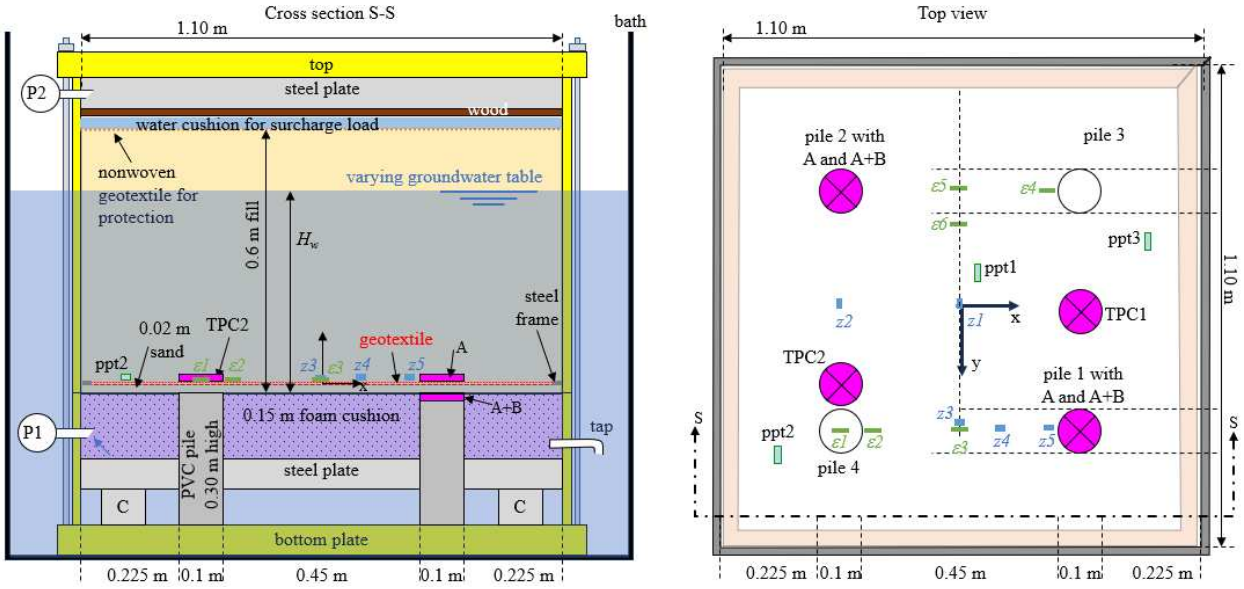

Figure 1. Test setup GRPS embankment in bath to induce a varying groundwater table in the fill.

2 SCALED EXPERIMENTS

Figure 1 shows the test setup (van Eekelen et al., 2012a, 2024). A steel plate supports a foam cushion, that is sealed and soaked. A tap allows for the drainage of the foam cushion. Four PVC piles with a 0.1 m diameter pass through the steel plate.

Two layers of Geolon 100-50 woven geotextile were placed perpendicular to and directly on top of each other. They were attached to a rigid steel frame. The combined geotextiles had a tensile strength of 100+50 = 150 kN/m and a tensile stiffness at 2% strain of $J_{2\%}$ = 1200 kN/m and 1013 kN/m for 10 and 1000 hours loading, respectively.

An equally distributed surcharge load was applied on the fill surface, using a water cushion. A rubber sheet greased with Vaseline minimised the wall-soil friction. The load distribution in the fill was measured by total pressure cells, GR deflection with a liquid levelling system (water pressure cells in a tube filled with water and connected to a reference box with water), and the GR strains were measured using cables (van Eekelen et al., 2024).

Two types of mixed demolition waste granulate were used; one with fine content (d/D = 0/31.5 mm) and one without fine content (d/D = 4/31.5 mm), where d and D are the lower and upper sieve sizes (EN13242, 2015). Table 1 lists fill details. The values of $\varphi'_{15\%}$ were obtained from four drained large-scale triaxial tests with a sample diameter of 0.45 m.

Table 1. Test details of the three small-scale tests.

Test no.	1	2	3
Fill height above steel (m)	0.65	0.60	0.60
Limiting sieve sizes d/D (mm/mm)	4/31.5	0/31.5	4/31.5
Median particle size D_{50} (mm)	18.8	7.0	18.8
Unit weight dry fill γ_d (kN/m^3)	13.19	14.60	13.20
Unit weight saturated fill γ_s (kN/m^3)	18.11	19.00	18.12
Unit weight initial fill γ_i (kN/m^3)	13.90	15.39	13.91
Porosity n (V_{pores}/ V_{total})	0.50	0.45	0.50
Friction angle unsaturated fill $\varphi'_{15\%}$ (°)	41.0	39.4	41.0
Friction angle saturated fill $\varphi'_{15\%}$ (°)	40.5	39.6	40.5

After the installation of the reinforcement, sensors and the fill, the box was closed and placed in a bath (Figure 1). Then, the subsoil support was removed by sucking the foam cushion vacuum.

Subsequently, the bath was filled. The groundwater table in the fill followed the water level in the bath easily. Then, (in Tests 2 and 3) the groundwater table was lowered again. After that, the surcharge load was increased in steps. After each surcharge load step, a groundwater cycle was applied again. In Test 1, the phreatic line was kept constant.

3 CALCULATIONS

The three main European design methods for GRPS embankments are:

- the Concentric Arches model of van Eekelen et al., (2013, 2015, adopted in CUR226, 2016);
- the model of Zaeske (2001), adopted in EBGEO, (2011);
- the model of Hewlett and Randolph (1988) adopted in both the French ASIRI (2012) and the British Standard (BS8006, 2010).

The first calculation step of these models divides the vertical load into two parts (Figure 2). Part A (kN/pile) is directly transferred to the piles and is relatively large, due to soil arching. The residual load, 'B+C' (kN/pile) is supported by the subsurface between the piles.

The second calculation step calculates the GR strain, and implicitly also divides B+C further into B and C. In the tests presented in this paper, the foam cushion underneath the GR was sucked vacuum, so that for all tests the subsoil support was zero during the entire test, so that C = 0.

3.1 Input parameters

Figure 1 gives the geometry properties, and Table 1 the fill properties. The groundwater table H_w was derived from the measured pore pressures (ppt 1, 2 and 3). The weighted value of γ in equations (2) to (5) was derived from γ_d below groundwater level (combined with Archimedes' p_{uplift} for the grains) and γ_i (kN/m^3) above groundwater level. γ_i is the initial fill unit weight that includes the 5.4% moisture content of the sand above the phreatic line.

The wall-soil friction R was 20-25% of the total load and was derived by subtracting the measured A+B+C from the total effective load. R was subtracted from the surcharge load. There was no subsoil support, so the subgrade reaction k = 0 kN/m^3. The geotextile tensile stiffness $J_{2\%}$ was chosen in line with the test duration: $J_{2\%}$ = 1106 kN/m.

3.2 Water in the calculations

Archimedes' principle states that a body immersed in a fluid is subject to an upward force equal to the weight of the displaced fluid. This aligns Terzaghi's effective stresses, which are the difference between the total stress and the water pressure.

In this paper, Archimedes' upward pressure (p_{uplift}) is used to bring into account the water in the fill. This upward pressure is defined as:

$$p_{uplift} = (1\text{-}n) \cdot H_w \cdot \gamma_w \text{ (kPa)} \quad (1)$$

where n (-) is the porosity, H_w (m) is the groundwater table above the piles, and γ_w is the unit weight of water (9.81 kN/m^3).

This p_{uplift} is integrated in the CA calculations by reducing surcharge load p with p_{uplift}. Theoretically, this aligns Terzaghi's effective stress calculations. However, using the Terzaghi's effective stresses is not possible for the CA model. This is explained as follows for the CA model (van Eekelen et al., 2013), but also applies for EBGEO:

Firstly, the CA model calculates the load distribution A% and (B+C)% without including the surcharge load (p = 0). This results in $A_{p=0}$ and $(B+C)_{p=0}$. So far, the calculation only uses the soil weight above the arches (besides geometry and material properties). Therefore, using Terzaghi's effective stress-approach would only impact the calculation for the fill part above the arches.

Secondly, the CA model includes the surcharge load:

$$A_{p>0} = \frac{\gamma H+p}{\gamma H} \cdot A_{p=0} \text{ and} \quad (2)$$

$$(B+C)_{p>0} = \frac{\gamma H+p}{\gamma H} \cdot (B+C)_{p=0} \quad (3)$$

In this study, we account for the groundwater by adjusting the equations as follows:

$$A_{p>0} = \frac{\gamma H+p-p_{uplift}}{\gamma H} \cdot A_{p=0} \text{ and} \quad (4)$$

$$(B+C)_{p>0} = \frac{\gamma H+p-p_{uplift}}{\gamma H} \cdot (B+C)_{p=0} \quad (5)$$

4 IMPACT GROUNDWATER

4.1 Impact groundwater on soil arching

Figure 2 compares the measured and calculated soil arching for Test 2. We observe the following:

- A rising groundwater level gives a limited decrease in both A and B.
- This decrease is primarily attributed to the uplift forces of Archimedes' principle rather than a change in soil arching. This is demonstrated by the calculations, which closely match the measurements. The calculations included the Archimedes uplift but did not reduce the soil arching due to a higher groundwater level.
- Figure 2c shows a slight decrease in soil arching A% due to groundwater. This shows that the decrease in A is not solely attributable to the Archimedes uplift, even though this remains the most significant mechanism at play.

The soil arching almost immediately rebounds when the phreatic line decreases. The soil arching (A)

changes less than 3.5% due to groundwater cycles, both up and down. The only exception is the first groundwater cycle which decreases the arching by 26%. At that stage, the arching had not found its equilibrium yet.

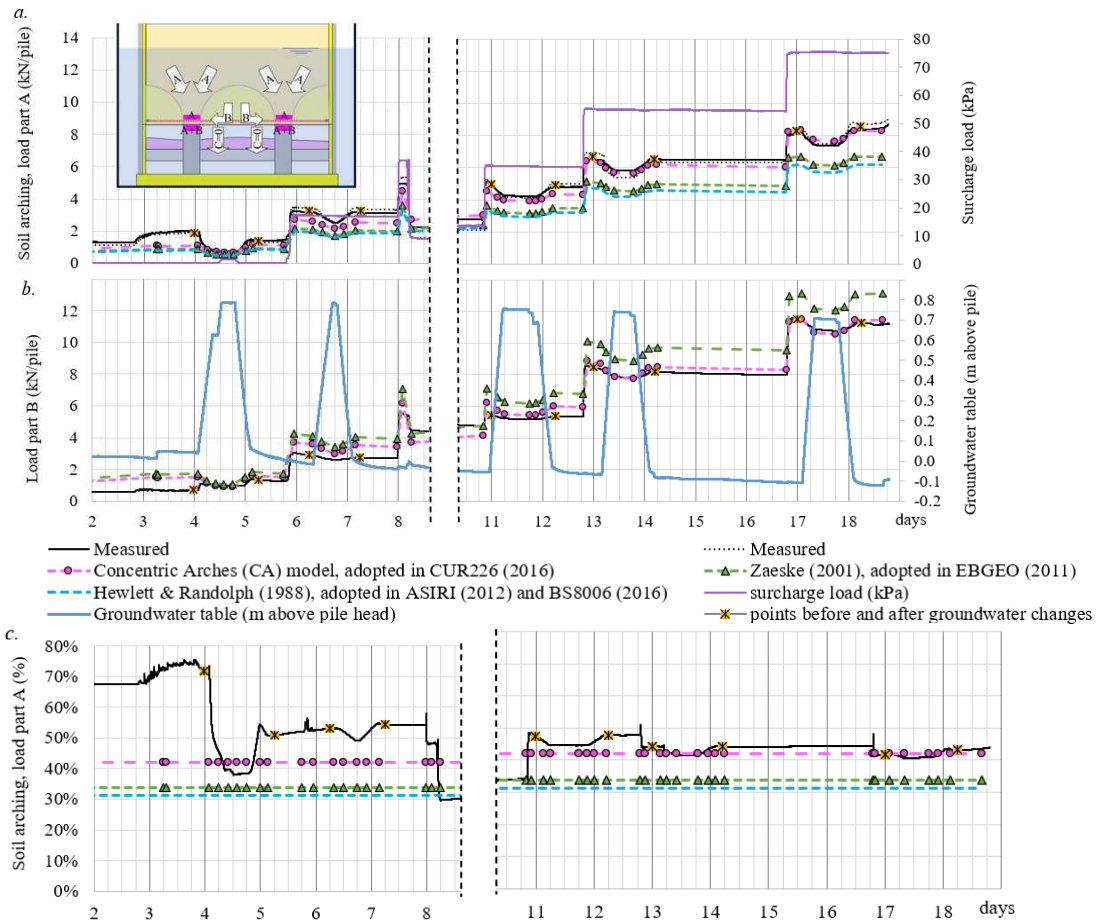

Figure 2. Comparison measured and calculated load distribution for Test 2. a. Soil arching (load part A). b. Load part B. c. Load part A in % of the total load. The 'measured' value of B was derived from the average measured values of A+B and A. p_{uplift} was integrated in all calculations by reducing surcharge load p with p_{uplift}. Between days 8 and 11, the surcharge load cushion leaked.

- The CA model matches the measurements better than the other two calculation models. Both EBGEO and Hewlett and Randolph (1988) underestimate the soil arching.

4.2 Impact groundwater on GR strains

Strain cables ('strain' or 'ε'), made from bicycle brake cables, were attached to the geotextile using tie wraps. The twisted steel wire that runs through an outer sleeve was pulled out by roughly 10 mm and fixed to the geotextile. A displacement transducer registered the difference between displacement of the twisted steel wire and the outer sleeve. This system provides only a qualitative result: many measured values are unrealistically large (van Eekelen et al., 2024): larger than the rupture strain, without rupture observed. Nevertheless, the measurements seem qualitatively reliable as in Figure 3a and Table 2, they match our expectations: the highest GR strains were measured in the strips between adjacent piles. The closer to the pile, the higher the strain. Outside the GR strip between adjacent piles (ε6), we observe much lower strains, typically around zero.

The GR strains do not show any significant response to changes in the groundwater level. This matches the findings of van Eekelen et al., 2023, who also found no convincing correlation between water and GR strain in field measurements. Temperature appeared to show a stronger correlation with the GR strain.

4.3 Impact groundwater on settlements

Figure 3b compares the measured and calculated GR deflection at the midpoint between two piles. The calculations were done for the middle of two adjacent piles. The CA model matches the measured deflection

nicely. Some settlement transducers show heave due to rising groundwater, specifically sensor z2. The calculations also show this effect, although to a lesser extent.

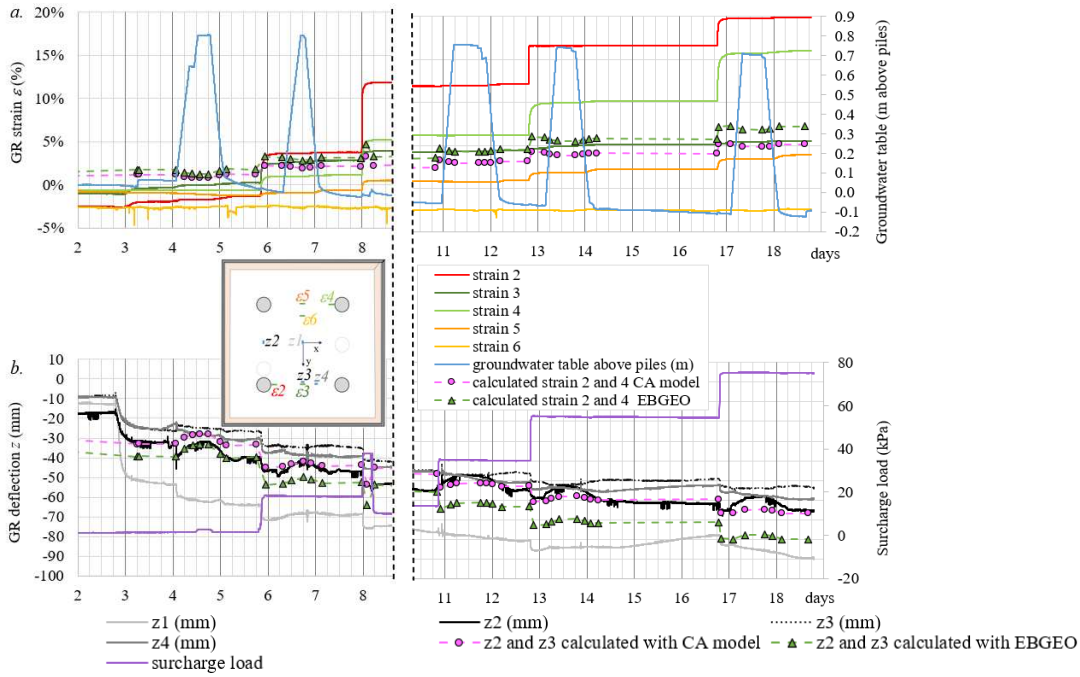

Figure 3. Measured and calculated deformations and strains. a. GR strains ε, and b. GR deflection z.

5 FILL WITH FINES OR NO FINES

Table 2 compares the measured and calculated values for Tests 1 to 3, for two surcharge loads (~ 17 and 55 kPa) and with and without groundwater.

The loading patterns of Tests 2 and 3 were comparable (after each surcharge load step a groundwater cycle), while Test 1 had surcharge load steps during one high groundwater period.

The deformations of Tests 2 and 3 match well, both with each other and with the CA calculations. The fill difference does not seem to have an impact.

The measured values of load part A, however, seem too high in the fill without fines of Tests 1 and 3. This difference is not in line with the measured GR deflections. Possibly, the issues that arose during Tests 1 and 3 play a role, such as leaks and malfunctioning sensors and pressure vessels. However, the high values of A in Tests 1 and 3 remain not fully explained.

As explained in Section 2, the strain measurements should only be considered qualitatively, they tend to be too large, sometimes larger than the rupture strain. In the average values of Table 2, these high values were not included.

All tests respond similarly to groundwater rise: a reduction in load and GR deflection, with a quick rebound after the high-water period. The CA calculations match the impact of groundwater well, if the uplift forces are taken into account.

Table 2. Comparison measurements and calculations for Tests 1, 2 and 3.

		Test 1	**Test 2**	**Test 3**	**Test 1**	**Test 2**	**Test 3**	**Test 1**	**Test 2**	**Test 3**	**Test 1**	**Test 2**	**Test 3**
	Time (day)	7.00	7.90	10.83	8.50	6.80	11.75	N/A	16.00	17.75	10.18	13.42	19.00
	Water table (m above pile)	0.00	0.00	0.00	0.65	0.60	0.55	N/A	0.00	0.00	0.65	0.60	0.60
	Surcharge load (kPa)	17.0	16.7	17.7	17.1	16.8	17.2	N/A	54.5	56.7	54.5	55.0	56.6
A (kN/pile)	Measured	4.9	3.2	4.6	3.7	2.5	3.7	N/A	6.4	9.1	7.7	5.6	8.5
	CA model (CUR226)	2.7	2.5	2.7	2.4	2.2	2.2	N/A	6.1	6.6	7.0	5.7	6.1
	Zaeske (EBGEO)	2.3	2.0	2.2	2.0	1.7	1.8	N/A	4.9	5.3	5.8	4.6	4.9
	Hewlett & Randolph 1988	2.2	1.9	2.0	1.9	1.6	1.6	N/A	4.5	4.9	5.6	4.2	4.5
GR deflection between two piles	Measured [1]	-43	-40	-37	-51	-38	-37	N/A	-55	-51	-67	-53	-52
	CA model (CUR226)	-44	-44	-44	-42	-42	-41	N/A	-60	-60	-61	-58	-58
	Zaeske (EBGEO)	-52	-52	-52	-50	-50	-49	N/A	-71	-72	-72	-70	-70
GR strain between two piles	Measured [2]	-	2.6%	1.6%	-	2.4%	1.6%	N/A	5.9%	3.0%	-	5.6%	3.1%
	CA model (CUR226)	2.1%	2.1%	2.1%	1.9%	1.9%	1.8%	N/A	4.1%	4.1%	4.2%	3.9%	3.9%
	Zaeske (EBGEO)	3.1%	3.1%	3.1%	2.8%	2.8%	2.7%	N/A	5.8%	5.8%	5.9%	5.5%	5.5%

[1] *Test 1: z4, Tests 2 and 3: average of z1, z2, z3.*

[2] *Clearly wrong measured strain values excluded (i.e. negative strain values and > 10%)*

6 CONCLUSIONS

Experiments were conducted to investigate the impact of groundwater in a GRPS embankment. The following conclusions were drawn:

- Groundwater gives a reduction of load, due to uplift forces.
- The reduction of load part A, which expresses soil arching, is mainly caused by the uplift forces, but a groundwater increase also leads to a slight reduction in soil arching.
- The soil arching immediately recovers when the groundwater level decreases again.
- The CA model provides a closer match to the measurements than the other two considered calculation models (EBGEO and Hewlett and Randolph (1988)), both of which underestimate the soil arching.
- The response on groundwater rise is similar for both fill types, with and without fines.
- An increase of groundwater gives some heave of the GR, due to the uplift forces. This heave disappears upon lowering the groundwater again.
- The presented experiment did not reveal any significant response of GR strains to changes in groundwater. This is in line with the field measurements of van Eekelen et al., 2023, who observed a correlation between air temperature and GR strain, and not between the groundwater table and GR strain. However, some authors, like Briançon and Simon (2012) and van Eekelen et al. (2020) reported changes in deformation and load distribution after heavy rain. It is possible that changes in temperature resulting from such heavy rain showers played a role in those cases, or by swelling of the subsoil due to the increase in water content.

ACKNOWLEDGEMENTS

The authors are grateful for the support of Solmax-TenCate, both financially and practically, and the support of the TKI-PPS funding of the Dutch Ministry of Economic Affairs.

REFERENCES

ASIRI (2013). *Recommendations for the design, construction and control of rigid inclusions ground improvements* (French version is of 2012).

Archimedes. (circa 250 BCE). Archimedes' Principle.

Briançon, L. and Simon, B. (2012). Performance of Pile-Supported Embankment over Soft Soil: Full-Scale Experiment, *J. of Geotech. and Geoenv. Eng.*, 138: 551-561. DOI: 10.1061/(ASCE)GT.1943-5606.0000561.

BS8006-1 (2010). Code of practice for strengthened/reinforced soils and other fills. British Standards Institution, UK.

CUR226 (2016). See Van Eekelen and Brugman (2016).

Hewlett, W.J. and Randolph, M.F. (1988). Analysis of piled embankments. Ground Eng. 21(3): 12-18.

NEN-EN 13242 (2015) *Hydraulic bound and unbound aggregates*.

Song, J., Chen, K., Li, P., Zhang, Y. and Sun, C. (2018). Soil arching in unsaturated soil with different water table. *Granular Matter*, 20: 78. DOI: 10.1007/s10035-018-0849-3.

van Eekelen, S.J.M., Bezuijen, A., Lodder, H.J. and van Tol, A.F. (2012a). Model experiments on piled embankments Part I. *Geotextiles and Geomembranes*, 32: 69-81. DOI: 10.1016/j.geotexmem.2011.11.002.

van Eekelen, S.J.M., Bezuijen, A. van Tol, A.F., (2013). An analytical model for arching in piled embankments. Geotextiles and Geomembranes 39: 78-102. DOI: 10.1016/j.geotexmem.2013.07.005.

van Eekelen, S.J.M., Nancey, A., Bezuijen, A. (2012b). Influence of fill material and type of geosynthetic reinforcement in a piled embankment, model experiments. In: *Proc. Eur. Geosynthetic Congres.,* Valencia, Spain, Vol 5, 167-171.

van Eekelen, S.J.M., Bezuijen, A. and Van Tol, A.F. (2015). Validation of analytical models for the design of basal reinforced piled embankments. *Geotextiles and Geomembranes*, 43(1): 56 - 81. DOI: 10.1016/j.geotexmem.2014.10.002.

van Eekelen, S.J.M. and Brugman, M.H.A., Eds. (2016). *Design Guideline Basal Reinforced Piled Embankments* (CUR226). CRC Press, Delft, Netherlands.

van Eekelen, S.J.M., Venmans, A.A.M., Bezuijen, A. and van Tol, A.F. (2020). Long term measurements in the Woerden geosynthetic-reinforced pile-supported embankment. *Geosynthetics International,* 27(2): 142-156. DOI: 10.1680/jgein.17.00022.

van Eekelen, S.J.M., Zwaan, R.A., Nancey, A., Hazenkamp, M. and Jung, Y.H. (2023). Four years field measurements in a partly submerged woven geotextile-reinforced pile-supported embankments. *Geosynthetics: Leading the Way to a Resilient Planet*, 1072-1077. DOI: 10.1201/9781003386889-133

van Eekelen, S.J.M., Wittekoek, B., Zwaan, R.A., Bezuijen, A., Nancey, A. (2024). 3D Experiments in bath: groundwater in geosynthetics-reinforced pile-supported embankments. In: *Proc. ECPMG 2024,* Delft, Netherlands.

Wang, H.-L., Chen, R.-P., Cheng, W., Qi, S. and Cui., Y.-J. (2018). Full-scale model study on variations of soil stress in geosynthetic-reinforced pile-supported track bed with water level change and cyclic loading. *Can. Geot. J.* 56(1): 60-68. DOI: 10.1139/cgj-2017-0689.